Sum-Rate Capacity of Random Beamforming for Multi-Antenna Broadcast Channels with Other Cell Interference

Sung-Hyun Moon, Sang-Rim Lee, and Inkyu Lee, *Senior Member, IEEE*

***Abstract*—In this letter, we analyze the sum rate of random beamforming (RBF) for downlink multi-antenna systems in the presence of other cell interference (OCI). Employing extreme value theory, an expression of the asymptotic ergodic sum rate with a large number of users is derived from the limiting distribution of the sample maximum of the received signal-to-interference-plus-noise ratio. Based on our result, the scaling law of multiuser diversity gain is also exhibited in the context of RBF systems with the OCI, which is shown to coincide with the previous result without the other cell interferers. Simulation results verify the validity of our analysis even with not so large number of users.**

***Index Terms*—MIMO broadcast channel, random beamforming, multiuser scheduling, other-cell interference.**

I. Introduction

FOR next generation wireless systems, significant research efforts have been devoted to multiple-input multiple-output (MIMO) techniques, which can attain substantial capacity gains [1]–[4]. In order to improve the information rate, a variety of precoding schemes have been proposed for multiuser systems including optimal dirty paper coding (DPC) [5] and simple linear beamforming methods [6]–[8]. However, the actual performance promised by the MIMO techniques can be severely degraded in a realistic cellular system. Especially, cell edge users experience poor throughput performance due to severe signal attenuation and other cell interference (OCI) coming from neighboring base stations (BSs). Hence, dealing with the OCI problem has become one of the most important design issue for future cellular standards [9]. Another fundamental limit in the real-world system design is the feedback overhead. In frequency division duplex systems, channel state information (CSI) should be quantized to be fed back, which incurs inevitable capacity loss resulting from quantization error. Currently, numerous related works addressing limited feedback strategies are in progress for various system configurations [10].

Random beamforming (RBF) is one of effective techniques for MIMO downlink channels which takes advantage of its simple structure and small feedback load [11]. It was shown in [11] that the RBF achieves the same optimal sum rate growth as the DPC. Also in practice, simple RBF approach, such as per user unitary and rate control (PU2RC), can outperform zero-forcing beamforming when the number of users K is large [12]. Recently, there have been efforts to better understand the capacity behavior of the RBF by studying the asymptotic regime of large K [12]–[14]. However, the effect of the other cell interferers was not taken into account in the prior works.

In this letter, we analyze the sum rate performance of the RBF systems in the presence of the OCI. An exact sum rate is difficult to compute, since the distribution of the received signal-to-interference-plus-noise ratio (SINR) is quite complicated to deal with. Thus, employing the theory of extreme order statistics, we derive an asymptotic closed-form expression on the ergodic sum rate for a large K. From our analysis, we also find that the sum rate of the RBF scales as $M_s \log_2 \log_2 K$ with arbitrary power level of the OCI signals when supporting M_s users at a time. Numerical results show that our derivation is quite accurate even for a small number of users.

Throughout this letter, we use the following notations. Normal letters represent scalar quantities, bold face letters indicate vectors, and boldface uppercase letters designate matrices. The superscript $(\cdot)^H$ stands for the Hermitian transpose and the expectation of a random variable is given by $\mathbb{E}(\cdot)$.

II. System Description

A. System model

Consider a multiuser multiple-input single-output (MISO) downlink channel where a BS with M antennas communicates to K single antenna users. Among K users, M_s users ($M_s \leq M$) are selected via multiuser scheduling in each transmission. We assume that there exist L cochannel interferers for each user from neighboring cells. First, we define the precoded signal vector $\mathbf{s} \in \mathbb{C}^{M\times 1}$ as $\mathbf{s} = \sum_{j=1}^{M_s} \mathbf{w}_j u_j$ where u_j denotes the complex-valued transmit data symbol given as $u_j = u_{j,I} + \sqrt{-1}u_{j,Q}$ and $\mathbf{w}_j \in \mathbb{C}^{M\times 1}$ is the beamforming vector for the symbol u_j. In the same way, the l-th OCI signal vector ($l = 1, \cdots, L$) is given by $\overline{\mathbf{s}}_l = \sum_{j=1}^{M_s} \overline{\mathbf{w}}_{l,j}\overline{u}_{l,j}$. Throughout this letter, we use the bar notation to represent the terms related to the OCI. We assume that each BS satisfies the sum power constraint P.

Then, the received signal y_k of user k is written as

$$y_k = \sqrt{a_k}\mathbf{h}_k^H\mathbf{s} + \sum_{l=1}^{L}\sqrt{\overline{a}_{k,l}}\,\overline{\mathbf{h}}_{k,l}^H\overline{\mathbf{s}}_l + n_k \tag{1}$$

where $\mathbf{h}_k \in \mathbb{C}^{M\times 1}$ and $\overline{\mathbf{h}}_{k,l} \in \mathbb{C}^{M\times 1}$ indicate the desired and the l-th OCI Rayleigh fading channel vector for user

Manuscript received November 30, 2010; revised February 10, 2011; accepted June 3, 2011. The associate editor coordinating the review of this letter and approving it for publication was H. Jafarkhani.

The authors are with the School of Electrical Engineering, Korea University, Seoul, Korea, 1, 5-Ga, Anam-Dong, Seongbuk-Gu, Seoul 136-713, Korea (e-mail: {shmoon, sangrim78, inkyu}@korea.ac.kr).

This work was supported in part by the National Research Foundation of Korea (NRF) grant funded by the Korea Government (MEST) (No. 2010-0017909), and in part by Seoul R&BD Program(WR080951).

This paper was presented in part at the IEEE International Conference on Communications (ICC) in Budapest, Hungary, May 2011.

Digital Object Identifier 10.1109/TWC.2011.070711.102145

k, respectively, whose entries are independent and identically distributed (i.i.d.) complex Gaussian $\mathcal{CN}(0,1)$, a_k and $\overline{a}_{k,l}$ denote the signal attenuation from the serving BS and the l-th neighboring BS, respectively, and n_k stands for the additive white Gaussian noise (AWGN) with $\mathcal{CN}(0,1)$. For analytical tractability, we consider homogeneous users so that each user experiences the same attenuations $a_k = a$ from its serving BS and $\{\overline{a}_{k,1}, \cdots, \overline{a}_{k,L}\} = \{\overline{a}_1, \cdots, \overline{a}_L\}$[1] from the neighboring BSs. It is also assumed that the local CSI $\sqrt{a}\mathbf{h}_k$ and $\{\sqrt{\overline{a}_l}\overline{\mathbf{h}}_{k,l}\}_{l=1}^{L}$ is perfectly known at the k-th user. At every BS, the uniform power $\frac{P}{M_s}$ is allocated across the data streams.

B. Review of RBF techniques

The RBF utilizes M_s orthonormal vectors $\boldsymbol{\phi}_1, \cdots, \boldsymbol{\phi}_{M_s} \in \mathbb{C}^{M\times 1}$ so that $\mathbf{w}_m$ is set to $\mathbf{w}_m = \boldsymbol{\phi}_m$ $(1 \le m \le M_s)$, which are generated independently at each cell in a pseudo-random fashion. The beam vectors for the l-th neighboring cell are denoted by $\overline{\boldsymbol{\phi}}_{l,m} \in \mathbb{C}^{M\times 1}$ for $1 \le m \le M_s$.

At the receiver, all users compute the SINR values for each of M_s beams, and feed back the highest SINR along with its index $\hat{m}$. Considering both the intra- and inter-cell interference signals from our OCI model (1), the SINR values of the k-th user for $m = 1, \cdots, M_s$ are obtained as

$$\mathrm{SINR}_{k,m} = \frac{a|\mathbf{h}_k^H\boldsymbol{\phi}_m|^2}{\frac{M_s}{P} + a\sum_{j\neq m}|\mathbf{h}_k^H\boldsymbol{\phi}_j|^2 + \sum_{l=1}^{L}\overline{a}_l\sum_j|\overline{\mathbf{h}}_{k,l}^H\overline{\boldsymbol{\phi}}_{l,j}|^2}. \quad (2)$$

Then, based on the SINR feedback (2) from every user, the BS performs scheduling by assigning its m-th data stream to user $\hat{k}$ who reports the highest SINR such as

$$\hat{k} = \arg\max_{k=1,\cdots,K} \mathrm{SINR}_{k,m}.$$

Under the above scheduling policy at the BS, the achievable sum rate R_{sum} can be written as

$$\begin{aligned} R_{\text{sum}} &\approx \sum_{m=1}^{M_s}\mathbb{E}\left[\log_2\left(1+\max_{k=1,\cdots,K}\mathrm{SINR}_{k,m}\right)\right] \\ &= M_s\mathbb{E}\left[\max_{k=1,\cdots,K}\log_2\left(1+\mathrm{SINR}_{k,m}\right)\right]. \quad (3) \end{aligned}$$

Here, the approximation is due to a small probability that the SINR of a certain user may be the highest for more than one data stream [11]. However, since this probability is negligible if K is not very small, we can consider (3) as quite an accurate expression for R_{sum}.

III. Asymptotic Sum Rate Analysis

In this section, we develop an asymptotic formula for the sum rate described in (3). Define $\Omega_k \triangleq M_s\log_2(1+\mathrm{SINR}_{k,m})$ and its sample maximum as $\Omega_{(K)} = \max_{k=1,\cdots,K}\Omega_k$. Then, (3) can be simply represented as

$$R_{\text{sum}} = \mathbb{E}[\Omega_{(K)}]. \quad (4)$$

Clearly, our goal is to find the distribution of $\Omega_{(K)}$. For this matter, we first investigate the distribution of $\mathrm{SINR}_{k,m}$.

For convenience, (2) can be rewritten as

$$\mathrm{SINR}_{k,m} = \frac{aX}{\frac{M_s}{P} + aW + \sum_{l=1}^{L}\overline{a}_l\overline{W}_l} \quad (5)$$

where $X = |\mathbf{h}_k^H\boldsymbol{\phi}_m|^2$, $W = \sum_{j\neq m}|\mathbf{h}_k^H\boldsymbol{\phi}_j|^2$ and $\overline{W}_l = \sum_{j=1}^{M_s}|\overline{\mathbf{h}}_{k,l}^H\overline{\boldsymbol{\phi}}_{l,j}|^2$. Note that $X = |\mathbf{h}_k^H\boldsymbol{\phi}_m|^2$ is i.i.d. over both k and m with $\chi^2(2)$ distribution since $\boldsymbol{\phi}_1, \cdots, \boldsymbol{\phi}_{M_s}$ are orthonormal [11]. Hence, W and $\overline{W}_l$ follow $\chi^2(2M_s-2)$ and $\chi^2(2M_s)$ distribution, respectively.

In (5), we introduce the interference term V as $V \triangleq aW + \sum_{l=1}^{L}\overline{a}_l\overline{W}_l$. Since W and all $\overline{W}_l$'s are independent, we find that V is a weighted sum of independent Chi-square random variables, whose probability density function (PDF) is complicated to compute. Instead of finding the exact distribution of V, we utilize the result in [15] that V can be well approximated by the Gamma distribution

$$f_V(v;\alpha,\beta) \approx v^{\alpha-1}\frac{e^{-\frac{v}{\beta}}}{\beta^\alpha\Gamma(\alpha)} \quad (6)$$

where $\Gamma(\alpha)$ is the gamma function $\Gamma(\alpha) = \int_0^\infty t^{\alpha-1}e^{-t}dt$ and the parameters α and β are given by [15]

$$\alpha = \frac{\left((M_s-1)a + M_s\sum_{l=1}^{L}\overline{a}_l\right)^2}{(M_s-1)a^2 + M_s\sum_{l=1}^{L}\overline{a}_l^2} \quad (7)$$

$$\beta = \frac{(M_s-1)a^2 + M_s\sum_{l=1}^{L}\overline{a}_l^2}{(M_s-1)a + M_s\sum_{l=1}^{L}\overline{a}_l}. \quad (8)$$

In Figure 1 (a), we compare the Gamma cumulative distribution function (CDF) from (6) with the actual CDF of V obtained from simulations with $M = 4$. The weight coefficients a and $\overline{a}_1, \cdots, \overline{a}_L$ are uniformly generated between -10 dB and 0 dB and are fixed during the simulation. From this plot, we confirm that the approximation for V is quite accurate for various configurations.

Now, using the gamma PDF (6), (7) and (8), we can calculate the approximate PDF of $\mathrm{SINR}_{k,m}$ as

$$\begin{aligned} f_S(x) &= \int_0^\infty f_{X|V}(x|v)f_V(v;\alpha,\beta)dv \\ &\approx \int_0^\infty \frac{\frac{M_s}{P}+v}{a}e^{-\frac{\left(\frac{M_s}{P}+v\right)x}{a}}v^{\alpha-1}\frac{e^{-\frac{v}{\beta}}}{\beta^\alpha\Gamma(\alpha)}dv \\ &= \frac{\beta e^{-\frac{M_s x}{Pa}}}{a}\left(\frac{M_s x}{Pa} + \frac{M_s}{P\beta} + \alpha\right)\left(\frac{\beta x}{a}+1\right)^{-\alpha-1} \quad (9) \end{aligned}$$

where $f_{X|V}$ is from the $\chi^2(2)$ distribution of X for given V. Also, the corresponding CDF $F_S(x)$ can be computed from (9) as

$$\begin{aligned} F_S(x) &\approx \int_0^x e^{-\frac{M_s y}{Pa}}\left(\frac{M_s}{Pa}\left(\frac{\beta y}{a}+1\right) + \frac{\alpha\beta}{a}\right)\left(\frac{\beta y}{a}+1\right)^{-\alpha-1}dy \\ &= 1 - e^{-\frac{M_s x}{Pa}}\left(\frac{\beta x}{a}+1\right)^{-\alpha}. \quad (10) \end{aligned}$$

Figure 1 (b) shows that the derived CDF in (10) exhibits very good agreement with empirical results. For example, $M = 4$ case with $L = 6$ interferers was compared in this figure.

Since users are homogeneous, $\mathrm{SINR}_{k,m}$ are i.i.d. over all $k = 1, \cdots, K$. Then R_{sum} in (3) can be expressed as $R_{\text{sum}} = \frac{M_s}{\ln 2}\int_0^\infty \frac{1-F_S^K(x)}{1+x}dx$. However, this integration is not

[1] Naturally, each element $\overline{a}_{k,l}$ is distinct for different user locations and thus in general $\overline{a}_{1,l} \neq \cdots \neq \overline{a}_{K,l}$ for $l = 1, \cdots, L$. Instead, we assume that the 'set' of all attenuation coefficients $\{\overline{a}_{k,1}, \cdots, \overline{a}_{k,L}\}$ is identical for all users. This can roughly be realizable since the neighboring cells are usually located in circularly symmetric way.

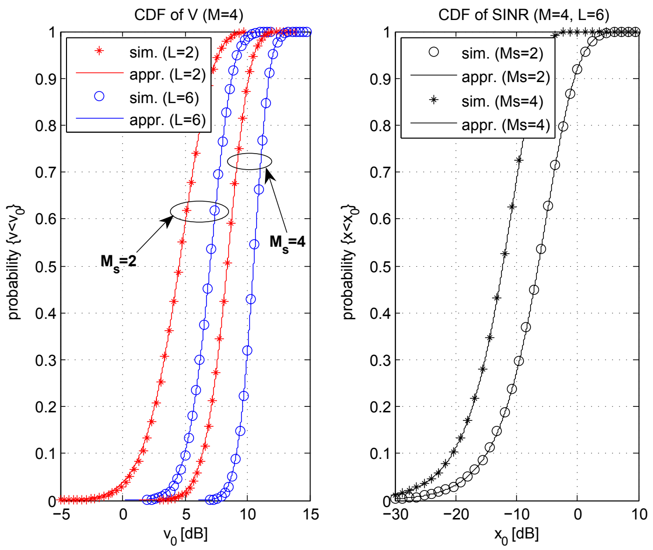

(a) CDF of V (b) CDF of $\text{SINR}_{k,m}$

Fig. 1. CDF comparison of V and $\text{SINR}_{k,m}$ for $M = 4$ and $M_s = 2$ and 4.

solvable with the CDF in (10). Even the high signal-to-noise ratio (SNR) approach used in [16] cannot be applied except $\frac{\beta}{a} = 1$ which never occurs in the presence of the OCI. Consequently, in this work, we attempt to evaluate R_{sum} in the asymptotic regime of large K. We need the following two lemmas to identify the asymptotic distribution of $\text{SINR}_{(K)}$.

Lemma 1: As $K \to \infty$, $\frac{\text{SINR}_{(K)} - \mu_S}{\sigma_S}$ converges to a standard Gumbel random variable whose PDF is $\exp(-e^{-x})$. The location and scale parameters μ_S and σ_S can be selected as

$$\mu_S = F_S^{-1}\left(1 - \frac{1}{K}\right) \tag{11}$$

$$\sigma_S = F_S^{-1}\left(1 - \frac{1}{Ke}\right) - \mu_S \tag{12}$$

where $F_S^{-1}(x) = \inf\{y : x \le F_S(y)\}$ represents the quantile function of the distribution of $\text{SINR}_{k,m}$.

Proof: For i.i.d. random variables, the main necessary condition for attraction to the Gumbel distribution is [17]

$$\lim_{x \to w(F)} \frac{d}{dx} \frac{1 - F(x)}{f(x)} = 0 \tag{13}$$

where $w(F) = \sup\{x : F(x) < 1\}$. From (9) and (10), it follows

$$\frac{d}{dx} \frac{1 - F_S(x)}{f_S(x)} = \frac{d}{dx} \frac{x + \frac{a}{\beta}}{\frac{M(x+\frac{a}{\beta})}{Pa} + \alpha} = \frac{d}{dx}\frac{Pa}{M} + O(x^{-1}) = O(x^{-2}). \tag{14}$$

Since $w(F) = \infty$, (14) converges to zero as $x \to w(F)$ and Lemma 1 is proved. ■

Lemma 2: For the parent distribution $F_S(x)$ given in (10), its quantile function $F_S^{-1}(y)$ is obtained by

$$F_S^{-1}(y) = \frac{P\alpha a}{M_s} W\left(\frac{M_s}{P\alpha\beta}(1-y)^{-\frac{1}{\alpha}} e^{\frac{M_s}{P\alpha\beta}}\right) - \frac{a}{\beta} \tag{15}$$

where $W(\cdot)$ is the Lambert W function [18].

Proof: For simplicity, we introduce $z = \frac{\beta x}{a}$. By substituting z into (10), we have

$$y = 1 - e^{-\frac{M_s z}{P\beta}} (z+1)^{-\alpha}.$$

Similar to the approach in [19], we can reformulate the above equation as the form of $v = we^w$ with $v = \frac{M_s}{P\alpha\beta} e^{\frac{M_s}{P\alpha\beta} - \frac{1}{\alpha}\log(1-y)}$ and $w = \frac{M_s}{P\alpha\beta}(z+1)$. Then, the variable x in (10) is represented by

$$x = \frac{a}{\beta} z = \frac{a}{\beta}\left(\frac{P\alpha\beta}{M_s} w - 1\right). \tag{16}$$

Noting that the solution of $v = we^w$ is $w = W(v)$, which is the definition of the Lambert W function, equation (16) can be derived as

$$\begin{aligned} x &= \frac{P\alpha a}{M_s} W(v) - \frac{a}{\beta} \\ &= \frac{P\alpha a}{M_s} W\left(\frac{M_s}{P\alpha\beta} e^{\frac{M_s}{P\alpha\beta} - \frac{1}{\alpha}\log(1-y)}\right) - \frac{a}{\beta} = F_S^{-1}(y) \end{aligned}$$

■

Lemma 1 and 2 show that as $K \to \infty$, the CDF of $\text{SINR}_{(K)}$ becomes $F_{S_{(K)}}(x) = \exp\left(-e^{-\frac{x-\mu_S}{\sigma_S}}\right)$, and its mean μ_S and variance σ_S^2 are determined by substituting (15) into (11) and (12). Now, we need to identify the asymptotic distribution of $\Omega_{(K)}$. We utilize a theorem provided in [20], named as *limiting throughput distribution (LTD) theorem*, which characterizes the limiting behavior of $\Omega_{(K)}$ without checking the condition (13) again for Ω_k.

Lemma 3: The distribution of Ω_k belongs to the domain of the attraction of the Gumbel distribution. The normalizing constants μ_Ω and σ_Ω are transformed from (11) and (12) into

$$\begin{aligned} \mu_\Omega &= M_s \log_2(1 + \mu_S) \\ \sigma_\Omega &= M_s \log_2(1 + (\mu_S + \sigma_S)) - \mu_\Omega. \end{aligned}$$

Proof: This lemma is a direct consequence of the LTD theorem [20]. ■

From Lemma 3, it follows that $\frac{\Omega_{(K)} - \mu_\Omega}{\sigma_\Omega}$ also falls into the standard Gumbel distribution in the asymptotic regime, which leads to our main result. Noting that the standard Gumbel distribution has the mean $\gamma_0 = 0.5772\cdots$ (Euler's constant), we have $\mathbb{E}\left[\frac{\Omega_{(K)} - \mu_\Omega}{\sigma_\Omega}\right] = \gamma_0$. Then, from (4), we finally arrive at an expression on the asymptotic ergodic sum rate R_{sum} as

$$\lim_{K\to\infty} R_{\text{sum}} = \mu_\Omega + \gamma_0 \sigma_\Omega \tag{17}$$

where μ_Ω and σ_Ω are given from Lemma 3 by

$$\mu_\Omega = M_s \log_2\left(\frac{P\alpha a}{M_s} W\left(\frac{M_s K^{\frac{1}{\alpha}}}{P\alpha\beta} e^{\frac{M_s}{P\alpha\beta}}\right) + \frac{\beta - a}{\beta}\right) \tag{18}$$

$$\sigma_\Omega = M_s \log_2\left(\frac{P\alpha a}{M_s} W\left(\frac{M_s (Ke)^{\frac{1}{\alpha}}}{P\alpha\beta} e^{\frac{M_s}{P\alpha\beta}}\right) + \frac{\beta - a}{\beta}\right) - \mu_\Omega \tag{19}$$

For the convergence proof of $\mathbb{E}[\Omega_{(K)}]$, one may refer to [20, Lemma 2].

If we set $\alpha = M_s - 1$ and $\beta = a$, the rate expression (17) reduces to the special case of no inter-cell interference, i.e., $\overline{a}_1 = \cdots = \overline{a}_L = 0$, from the relation of (7) and (8).

Although our analysis (17) holds in the asymptotic regime of $K \to \infty$, we will show in the next section that (17) is quite accurate even for the small number of users. We also note that for computing the Lambert W function, a couple of simple Newton's iterations are sufficient [18]. Nevertheless, $W(\cdot)$ can be further simplified using an approximation in [19] as

$$W(x) \approx c_1 \log_2(x + c_2) + c_3 \tag{20}$$

where c_1, c_2 and c_3 are fixed coefficients. This approximation is tight for $x > 0$, which is always met in our case. Using a usual curve-fitting method, the constants can be determined as $c_1 = 0.4264$, $c_2 = 0.6683$ and $c_3 = 0.2547$.

By applying the approximation (20) to our result, μ_Ω and σ_Ω can be expressed by simple log functions and therefore R_{sum} in (17) can be evaluated as a closed-form approximation. The final expression is not written again to avoid repetition. We find that our asymptotic expression is simpler than the previous analysis with finite K [13][21], and is relatively accurate compared to other bound approaches [14][19]. Now, we address the following observation.

Theorem 1: For fixed M_s and P, the sum rate (17) obeys the asymptotic growth rate as

$$\lim_{K\to\infty} \frac{R_{\text{sum}}}{M_s \log_2 \log_2 K} = 1. \tag{21}$$

Proof: Due to space limitation, we choose a simple and intuitive proof rather than a rigorous one. By inserting (20) into (18) and neglecting c_2 since $c_2 \ll K$, the limiting value of μ_Ω when $K \to \infty$ is given by

$$\begin{aligned}
&\lim_{K\to\infty} \mu_\Omega \\
&= \lim_{K\to\infty} M_s \log_2 \left(\frac{P\alpha a c_1}{M_s} \log_2 \left(\frac{M_s K^{\frac{1}{\alpha}}}{P\alpha\beta} e^{\frac{M_s}{P\alpha\beta}} \right) + O(1) \right) \\
&= \lim_{K\to\infty} M_s \log_2 \left(\frac{P a c_1}{M_s} \log_2 K + O(1) \right) && (22)\\
&= M_s \log_2 \log_2 K. && (23)
\end{aligned}$$

Next, from (22), the scale parameter σ_Ω can be shown to vanish as $K \to \infty$ as

$$\begin{aligned}
\lim_{K\to\infty} \sigma_\Omega &= \lim_{K\to\infty} M_s \log_2 \left(\frac{\frac{P\alpha a c_1}{M_s}(\log_2 K + \log_2 e) + O(1)}{\frac{P\alpha a c_1}{M_s} \log_2 K + O(1)} \right) \\
&= 0. && (24)
\end{aligned}$$

By putting (23) and (24) together into (17), we have (21). ■

Theorem 1 proves that R_{sum} scales as $M_s \log_2 \log_2 K$ over Rayleigh fading channels which is the optimal growth rate of ideal MISO broadcast channels with no inter-cell interference. One main assumption underlying the SINR expression in (2) is that the OCI signals are simply treated as noise. Therefore, we can see that in a purely distributed manner, the RBF technique fully exploits a multiuser diversity gain in the asymptotic regime of large K with any finite OCI signal powers $\overline{a}_{k,1}, \cdots, \overline{a}_{k,L}$.

IV. Simulation Results

In this section, we compare our sum rate analysis for MISO downlink RBF systems with numerical simulations to confirm the validity of our analysis. For simulations, we use spatially uncorrelated Rayleigh fading channels which are randomly and independently generated for each transmission. As explained before, each user feeds back the maximum SINR value and $\lceil \log_2 M_s \rceil$ bits for its index. As for the attenuation parameters, a is set to 0 dB and $\{\overline{a}_1, \cdots, \overline{a}_L\}$ are uniformly generated between -10 dB and 0 dB and fixed during the simulation. This setting roughly reflects the cell edge environment with strong OCI signals such that the users' signal-to-interference ratio might be considerably lower than 0 dB [9].

Figure 2 exhibits the average sum rate of the RBF with respect to K for $M = M_s = 4$ and $P = 10$ dB. Both the simulations and the analytical results based on (17) are plotted together in a wide range of $K \in [1, 100]$. The Lambert W function in (18) and (19) is calculated by (20). From this comparison, we emphasize that our analysis is consistent with

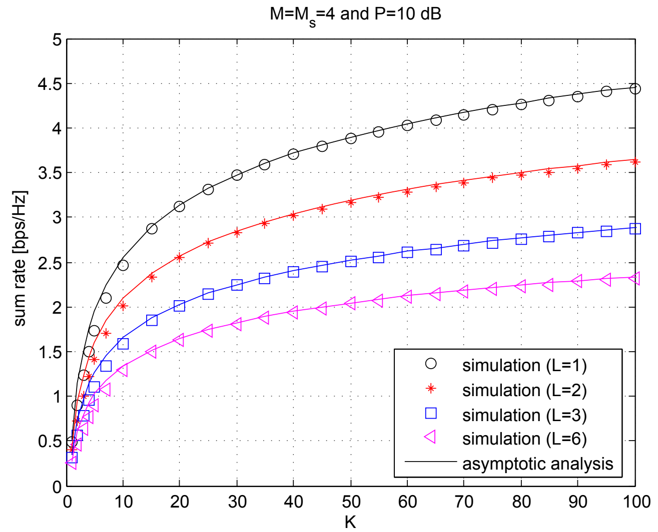

Fig. 2. Average sum rate of the RBF scheme for $M = M_s = 4$ and $P = 10$ dB.

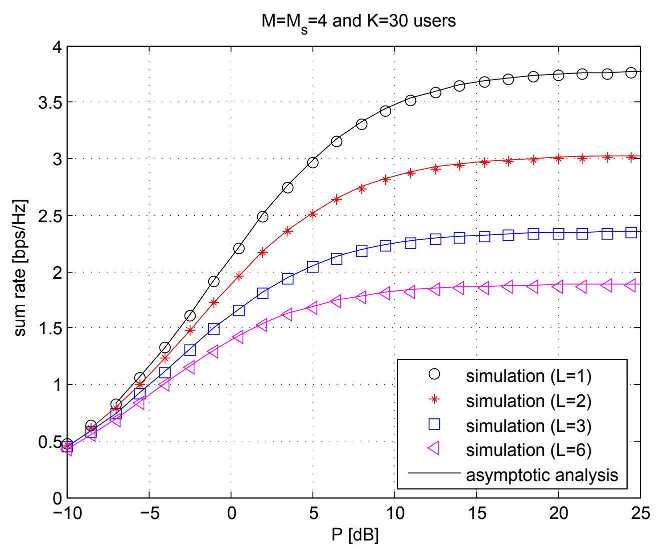

Fig. 3. Average sum rate of the RBF scheme for $M = M_s = 4$ with $K = 30$.

the empirical curves for various L and K, even with a small number of K. When K is very small, less than 10, we observe a slight discrepancy between our formula and the simulations. This is originated by the fact that when we define the sum rate in (3), we have ignored a small possibility that one user is scheduled for multiple data streams.

In Figure 3, we present the sum rates for $M = M_s = 4$ and $K = 30$ users with respect to P. We can see from this figure that our derived result (17) matches quite well with the actual sum rate performance over the whole range of SNRs for $L = 1, 2, 3$ and 6. From the two figures, we notice that the OCI causes a significant detrimental effect on the performance of RBF systems. This issue provides motivation for future studies of improved interference control strategies over the RBF based MIMO systems, which may include items such as joint intercell coordination schemes [22][23].

V. Conclusions

In this letter, we have analyzed the sum rate of the RBF technique for MISO downlink channels in the presence of the OCI. We have derived an expression of the ergodic sum rate when the number of users is asymptotically large. From numerical simulations, we have confirmed that our asymptotic analysis is valid for even small K. Also, our analysis reveals the sum rate scaling law $M_s \log_2 \log_2 K$ which generally holds regardless of the OCI strength.

References

[1] I. E. Telatar, "Capacity of multi-antenna Gaussian channels," *Eur. Trans. Telecommun.*, vol. 10, pp. 585-595, Nov. 1999.

[2] I. Lee, A. Chan, and C.-E. W. Sundberg, "Space-time bit-interleaved coded modulation for OFDM systems," *IEEE Trans. Signal Process.*, vol. 52, pp. 820-825, Mar. 2004.

[3] H. Lee, B. Lee, and I. Lee, "Iterative detection and decoding with an improved V-BLAST for MIMO-OFDM systems," *IEEE J. Sel. Areas Commun.*, vol. 24, pp. 504-513, Mar. 2006.

[4] H. Lee and I. Lee, "New approach for error compensation in coded V-BLAST OFDM systems," *IEEE Trans. Commun.*, vol. 55, pp. 345-355, Feb. 2007.

[5] G. Caire and S. Shamai, "On the achievable throughput of a multi-antenna Gaussian broadcast channel," *IEEE Trans. Inf. Theory*, vol. 49, pp. 1691-1706, July 2003.

[6] C. B. Peel, B. M. Hochwald, and A. L. Swindlehurst, "A vector-perturbation technique for near-capacity multiantenna multiuser communication—part I: channel inversion and regularization," *IEEE Trans. Commun.*, vol. 53, pp. 195-202, Jan. 2005.

[7] T. Yoo and A. Goldsmith, "On the optimality of multiantenna broadcast scheduling using zero-forcing beamforming," *IEEE J. Sel. Areas Commun.*, vol. 24, pp. 528-541, Mar. 2006.

[8] H. Sung, S.-R. Lee, and I. Lee, "Generalized channel inversion methods for multiuser MIMO systems," *IEEE Trans. Commun.*, vol. 57, pp. 3489-3499, Nov. 2009.

[9] J. G. Andrews, W. Choi, and R. W. Heath, "Overcoming interference in spatial multiplexing MIMO cellular networks," *IEEE Wireless Commun.*, vol. 14, pp. 95-104, Dec. 2007.

[10] D. J. Love, R. W. Heath, V. K. N. Lau, D. Gesbert, B. D. Rao, and M. Andrews, "An overview of limited feedback in wireless communications systems," *IEEE J. Sel. Areas Commun.*, vol. 26, pp. 1341-1365, Oct. 2008.

[11] M. Sharif and B. Hassibi, "On the capacity of MIMO broadcast channels with partial side information," *IEEE Trans. Inf. Theory*, vol. 51, pp. 506-522, Feb. 2005.

[12] K. Huang, J. G. Andrews, and R. W. Heath, "Performance of orthogonal beamforming for SDMA with limited feedback," *IEEE Trans. Veh. Technol.*, vol. 58, pp. 152-164, Jan. 2009.

[13] K.-H. Park, Y.-C. Ko, and M.-S. Alouini, "Accurate approximations and asymptotic results for the sum-rate of random beamforming for multi-antenna Gaussian broadcast channels," in *Proc. IEEE VTC*, Apr. 2009, pp. 1-6.

[14] M. Xia, Y. Zhou, J. Ha, and H. Chung, "Opportunistic beamforming communication with throughput analysis using asymptotic approach," *IEEE Trans. Veh. Technol.*, vol. 58, pp. 2608-2614, June 2009.

[15] A. H. Feiveson and F. C. Delaney, "The distribution and properties of a weighted sum of chi squares," NASA Technical Note D-4575, May 1968.

[16] E. A. Jorswieck, P. Svedman, and B. Ottersten, "Performance of TDMA and SDMA based opportunistic beamforming," *IEEE Trans. Wireless Commun.*, vol. 7, pp. 4058-4063, Nov. 2008.

[17] L. de Haan and A. Ferreira, *Extreme Value Theory: An Introduction*. Springer, 2006.

[18] R. M. Corless, G. H. Gonnet, D. E. G. Hare, D. J. Jeffrey, and D. E. Knuth, "On the Lambert W function," *Advances Computational Mathematics*, vol. 5, pp. 329-359, 1996.

[19] Y. Kim, J. Yang, and D. K. Kim, "A closed form approximation of the sum rate upperbound of random beamforming," *IEEE Commun. Lett.*, vol. 12, pp. 365-367, May 2008.

[20] G. Song and Y. Li, "Asymptotic throughput analysis for channel-aware scheduling," *IEEE Trans. Commun.*, vol. 54, pp. 1827-1834, Oct. 2006.

[21] J. Yang, Y. Kim, H. Chae, and D. K. Kim, "A closed form approximation of the sum rate of random beamforming with multiple codebooks and its application to control of the number of codebooks," *IEEE Commun. Lett.*, vol. 12, pp. 672-674, Sep. 2008.

[22] W. Choi and J. G. Andrews, "The capacity gain from intercell scheduling in multi-antenna systems," *IEEE Trans. Wireless Commun.*, vol. 7, pp. 714-725, Feb. 2008.

[23] D. Gesbert and M. Kountouris, "Resource allocation in multicell wireless networks: some capacity scaling laws," in *Proc. IEEE WiOpt—RAWNET*, Apr. 2007, pp. 1-7.